

Magnetic-field dependent differential capacitance of polymer diodes

Thaddee K. Djidjou, Tek Basel, and Andrey Rogachev

Department of Physics and Astronomy, University of Utah, Salt Lake City, Utah 84112, USA

(Received 23 July 2012; accepted 15 August 2012; published online 28 August 2012)

Using admittance spectroscopy, we found that bipolar organic diodes based on pi-conjugated polymer, 2-methoxy-5-(2'-ethylhexyloxy), MEH-PPV, have strong divergent contribution to the device differential capacitance. It is positive at low bias voltages, turns negative at intermediate biases, and becomes positive again at stronger biases. In addition, we found that at certain biases, a small magnetic field can change the capacitance from divergent negative to divergent positive. Possible physical processes responsible for this anomalous behavior of the capacitance and its relation to the phenomenon of organic magnetoresistance are discussed. © 2012 American Institute of Physics. [<http://dx.doi.org/10.1063/1.4748797>]

Recent transport and electroluminescence studies have shown that an external magnetic field can change the current and light output of organic light emitting diodes (OLEDs) with no ferromagnetic electrodes. The phenomenon is commonly referred to as organic magnetoresistance (OMAR); it is quite universal and since its discovery in 2003¹ has been observed in many organic diodes based on small molecules^{2,3} and π -conjugated polymers.^{2,4,5} The organic magnetoresistance can reach sizable value of 20% in a relatively small field on the order of 10 mT at room temperature. This property can be used for magnetic field sensors and can provide magnetic control of electronic and optical properties of organic devices. Understanding the OMAR response on both static and time-dependent magnetic and electric fields is beneficial for such applications. Several proposed theoretical models have identified possible elementary processes that can be affected by magnetic field and change the device conductance. In the polaron-polaron (PP) model, proposed by Prigodin *et al.*,⁶ it is assumed that electrostatically bound pairs of positive and negative polarons with singlet components have higher exciton formation rate compared to triplet pairs and as a result have higher recombination probability. External magnetic field suppresses hyperfine mixing between triplet and singlet components and thus decreases average recombination rate. This process allows for more carrier injection and results in an increase in the concentration of carriers and consequently in the current of the device.⁷ The current increase and positive magnetoconductance can also occur, as it was suggested by Hu and Wu,⁸ because singlet polaron pairs have higher dissociating rate. Recent electrically detected magnetic resonance (EDMR) studies of MEH-PPV-based OLEDs demonstrated that the manipulation of the spin state of PPs indeed changes the free-polaron density in the material with corresponding change in conductance.^{9,10} The second proposed mechanism of the OMAR considers reactions between triplet excitons and polarons (TEP mechanism).^{8,11} A triplet exciton can release a trapped polaron⁷ or can act as a blocking site for a free polaron¹² influencing the mobility of carriers. Both processes depend on a total spin of a triplet-exciton-polaron complex; the magnetic field affects the mobility by suppressing hyperfine mixing between 3/2 and 1/2 spin states of the complex. The presence of these states was recently detected by EDMR in

electron-rich, unbalanced MEH-PPV-based diodes.¹³ The mobility also changes with magnetic field within the bipolar (BP) mechanism, which unlike PP and TEP processes can take place in unipolar devices.¹⁴ In recent time-of-flight measurements, enhancement of the mobility of majority carriers (holes) with magnetic field was detected in MEH-PPV;¹⁵ however, in Alq₃, the mobility was found to be field-independent.¹⁶

EDMR measurements on MEH-PPV¹³ suggest that different mechanisms can dominate magnetoconductance in different regimes or take place concurrently. In recent admittance spectroscopy studies of bipolar MEH-PPV-based devices at low and intermediate biases, we found that admittance spectra are dominated by two relaxation processes with distinct time scales.¹⁷ In this letter, we report on behavior of these devices in high bias regime where we observed a remarkable “flip” effect, namely we found that the external magnetic field can flip the device capacitance from negative to positive.

Bipolar OLEDs used in the present study consist of multilayers having the structure ITO/PEDOT:PSS/MEH-PPV/Ca/Al, where ITO is indium tin oxide; PEDOT:PSS is poly(3,4-ethylenedioxythiophene):poly(styrene sulphonate), which forms a hole injection layer. The cathode was a 2 nm-thick Ca layer covered by an Al layer for oxidation protection. The surface area of the devices was about 1 mm². Overall 17 devices were studied; parameters of the devices used in this contribution are summarized in Table I. In device H, DOO-PPV (Poly[2,5-dioctyloxy-1,4-phenylenevinylene]) was used for the active layer. The admittance spectroscopy measurements were performed at ambient conditions using a home-made apparatus.

The device admittance is commonly analyzed as $Y(\omega) = G(\omega) + i\omega C(\omega)$, where $G(\omega)$ is the differential conductance and $C(\omega)$ is the differential capacitance. The dependence of $C(\omega)$ versus frequency is shown in Fig. 1 for device F, which has MEH-PPV thickness of 160 nm. At zero bias, the capacitance of the devices has a positive contribution that decreases with frequency. Such contribution is typically associated with traps in a system. At intermediate biases (between 4 and 5.6 V for device F), we can distinguish two negative contributions. One of them, C_1 , dominates at frequencies below 10 Hz and the other, C_2 , above 10 Hz.

TABLE I. Parameters of the devices.

	Material	Thickness (nm)
C	MEH-PPV	150
F	MEH-PPV	160
G	MEH-PPV	50
H	DOO-PPV	50

From the analysis of the $C(\omega)$ dependence,¹⁷ we found that the relaxation time associated with C_1 , $\tau_1 \approx 0.8$ s, does not depend on bias, whereas the time scale of the second process, τ_2 , approximately exponentially decreases with bias. As one can see from Fig. 1(a), both contributions, C_1 and C_2 , depend on magnetic field. The behavior of C_2 contribution is analyzed in details in Ref. 17.

The evolution of capacitance at bias voltages above 5.6 V is shown in Fig. 1(b). The relaxation time τ_2 continues to decrease in this regime. This can be seen from the fact that the frequency corresponding to intersection of $C(f)$ with zero-axis shifts to higher values with increasing bias. The change of C_1 term is more significant. In voltage range between 5.6 and 6.6 V, C_1 reverses its behavior from negative to positive. The reversal is robust; it was observed in all

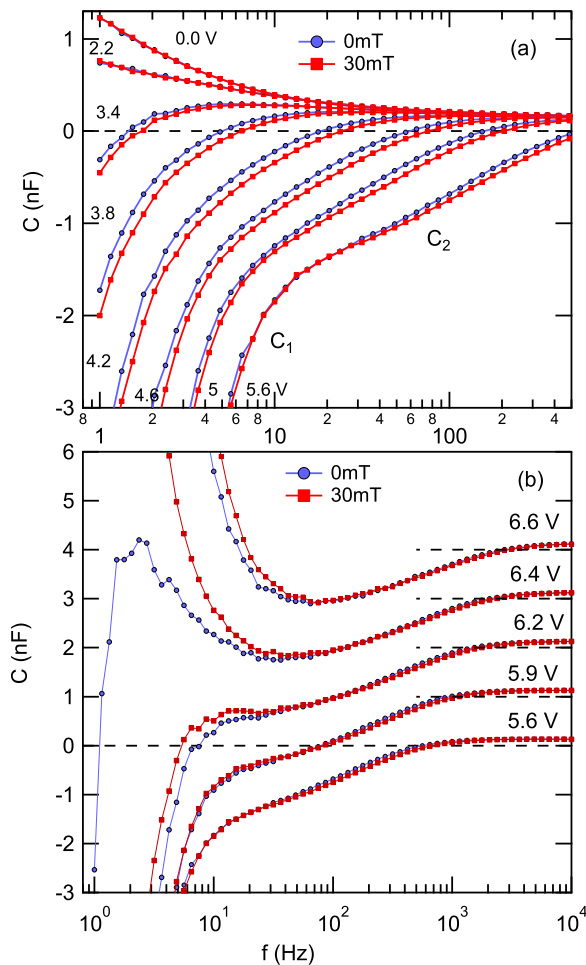


FIG. 1. Conductance of device F (thickness 160 nm) versus frequency. (a) Low and intermediate bias regimes. (b) High bias regime. The data for indicated bias voltages are shifted for clarity. Dashed lines indicate level of zero capacitance.

bipolar devices where high bias regime was tested. By carefully selecting bias voltage, we were able to tune some diodes to a state where the reversal could be induced by magnetic field only. An example of such a behavior is shown in Fig. 2 for device C with MEH-PPV thickness of 150 nm. When bias voltage $V_B = 7.10$ V and magnetic field is zero, the capacitance is negative and divergent. Application of magnetic field $B = 12$ mT makes the capacitance frequency-independent; at higher magnetic field, the capacitance again becomes divergent but positive.

Figures 1(b) and 2 indicate that the variation of capacitance with frequency right at the point of reversal can be complicated. However, away from this point at frequencies below 10 Hz, experimental data can be well fitted by the equation

$$C(\omega) = C_0 + \frac{C_{10}}{1 + \omega^2 \tau_1^2}, \quad (1)$$

which corresponds to an exponential relaxation with a single time constant.¹⁸ Here the term C_0 includes both the geometrical capacitance and contribution C_2 that is frequency-independent in this regime. From fitting of the data for several samples, we found that time constant τ_1 is approximately the same on negative and positive sides of the “flip.” For example, as shown in Fig. 2, Eq. (1) with the same parameters $C_0 = -500$ pF and $\tau_1 = 0.35$ s fits well both negative capacitance at $B = 0$ mT and positive capacitance at $B = 180$ mT. The values of C_{10} are -0.2 μ F for $B = 0$ mT and 0.12 μ F for $B = 180$ mT.

A typical evolution of the capacitance at fixed frequency (3 Hz) is shown in Fig. 3(a) for device G with MEH-PPV thickness of 50 nm. The inset in the figure shows the capacitance variation on the magnified scale. The magnitude of the capacitance is very high, particularly in thin samples. For diode G, it reaches the value of 100 nF at $V_B = 7$ V. The effect is even stronger in diode H, in which 50 nm-thick layer of DOO-PPV was used as an active layer (Fig. 3(b)). For this sample, the capacitance at $f = 1$ Hz and $V_B = 4.16$ V reaches 17 μ F, which is about 10^5 times larger than the geometrical

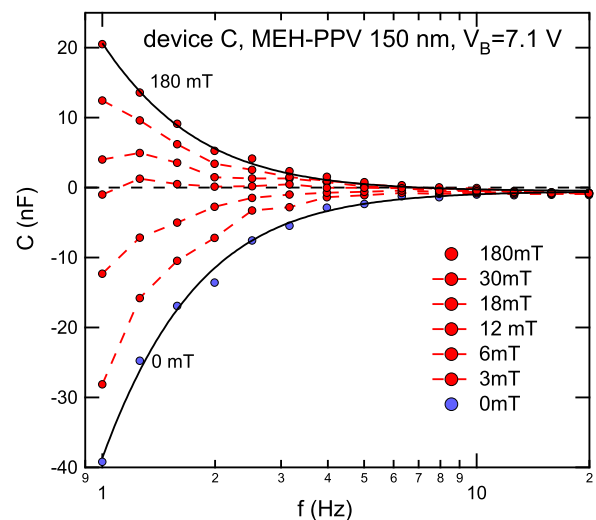


FIG. 2. Capacitance of device C (thickness 150 nm) at bias voltage 7.1 V versus frequency at indicated magnetic fields. The solid black lines are fits of the data at $B = 0$ and 180 mT with Eq. (1).

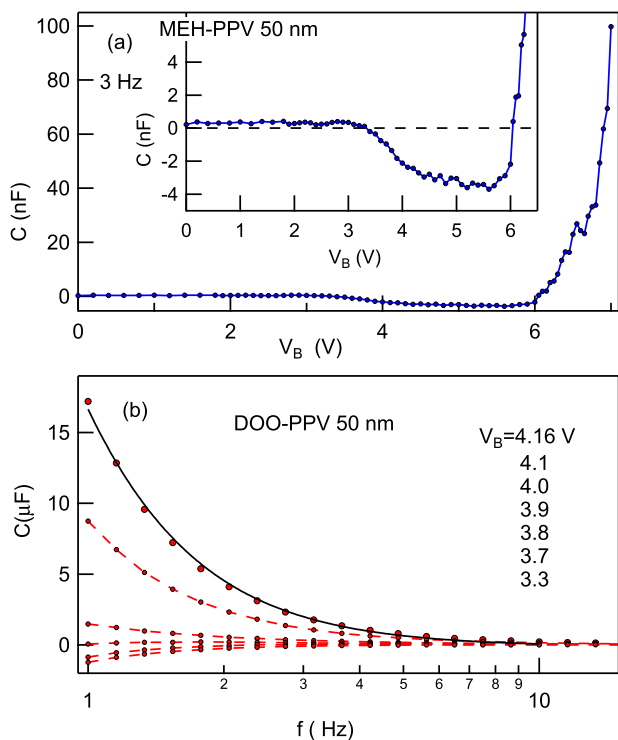


FIG. 3. (a) Capacitance at 3 Hz as a function of bias voltage for device G (MEH-PPV thickness is 50 nm). The inset shows the same data on the magnified scale. (b) Capacitance versus frequency at indicated biases for device H with 50 nm-thick DOO-PPV active layer. The solid line is a fit of the data at $V_B = 4.16$ V with Eq. (1).

capacitance. The data can be well approximated by Eq. (1); the fit is shown as a solid black line. The value of parameter C_{10} is 0.2 mF at $V_B = 4.16$ V. The time scale in DOO-PPV, $\tau_1 \approx 0.4$ s, is close to the value of τ_1 in MEH-PPV. The polymers have similar chemical structure and the detection of the same τ_1 suggests that C_1 contribution is likely related to trap states that are structurally and electronically identical in both materials.

Similar to our observation, a “positive-negative-positive” variation of the capacitance with increasing bias was detected by Bisquert *et al.*¹⁹ in OLEDs based on PPV co-polymer “super yellow.” In this work, the capacitance variation was attributed to the sequential electron injection via surface trap states formed at the PPV/Ba interface. In MEH-PPV OLEDs, we observed negative capacitance with the same time constant not only in bipolar devices but also in a unipolar device with the layer sequence ITO/PEDOT:PSS/MEH-PPV/Au.¹⁷ This suggests that if interface states are indeed responsible for C_1 , these should be states at the PEDOT:PSS/PPV interface. Efficiency of carrier injection from PEDOT:PSS is known to depend on chemical or ultraviolet light-ozone treatment,²⁰ so this material likely has electrically active surface defects. Within the model proposed by Bisquert *et al.*, negative capacitance occurs because the occupancy of intermediate interface states *decreases* with increasing bias. We notice that qualitatively similar effect may involve bulk traps, namely negative capacitance may occur if the occupancy of bulk trap states decreases with increasing bias. For example, this may happen if the trapped states act as centers of monomolecular recombination and the recombination rate grows with bias faster than the trapping rate.

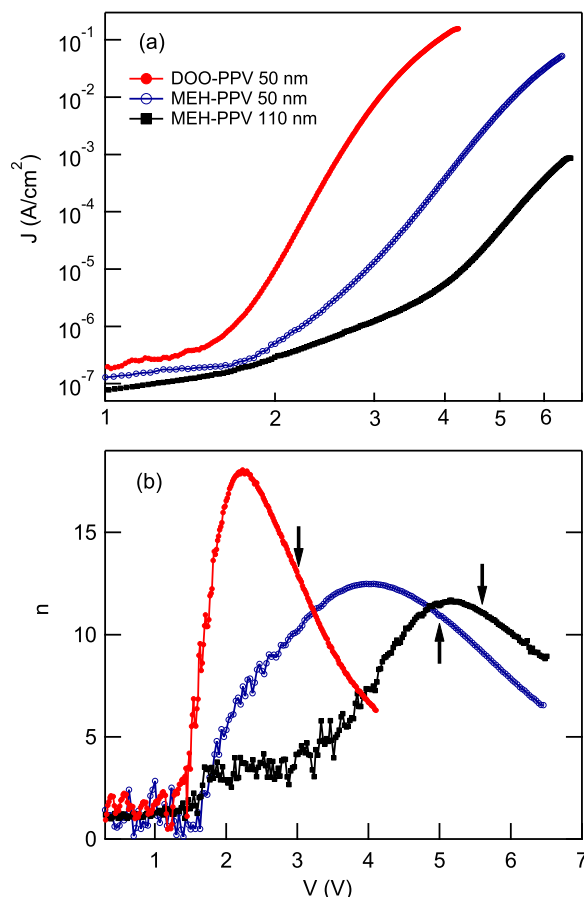


FIG. 4. (a) Current density versus frequency for several studied OLEDs. (b) The parameter $n = d(\ln(J))/d(\ln(V))$ as function of bias for the same OLEDs. Vertical arrows indicate biases at which the capacitance reverses from negative to positive.

In Fig. 4(a), we show current density versus bias for several studied OLEDs; panel (b) of the figure shows the variation of parameter $n = d(\ln(J))/d(\ln(V))$, which is equal to an exponent in a functional dependence $J \propto V^n$. As expected, for all diodes $n \approx 1$ in the ohmic regime at voltages below built-in potential $V_{BI} \approx 2$ V. At higher biases, n initially strongly increases with bias, then saturates, and starts to decrease. We found that in all studied diodes, the reversal of capacitance from negative to positive (indicated in the figure by arrows) systematically occurs at a voltage slightly above the maximum of n . The position of maximum and the reversal voltage shift to higher values with increasing device thickness. For bipolar space-charge limited diodes, i.e., diodes with ohmic contacts, parameter n is predicted to be in the range between 2 and 3.²¹ Much higher values of n are expected when the current is injection limited. (For example, the values of n in the range between 6 and 16 were found in $I(V)$ characteristics of injection-limited Alq₃-based OLEDs.²²) It is, therefore, possible that the saturation of n and the reversal of the capacitance in the MEH-PPV diodes are related to the transition from the injection-limited regime at low biases to the space-charge limited regime at high biases.

The dynamic charge transport in the bipolar MEH-PPV OLEDs is a complicated phenomenon that can be influenced by many processes: charge injection, interface states, bimolecular and trap-assisted recombination, and depolarization

of permanent dipoles.¹⁶ Surprisingly, the overall response of the admittance on *magnetic field* is very simple, at least phenomenologically. For all studied devices, we found that the application of magnetic field is equivalent to a small increase in the bias voltage. This can be illustrated using the capacitance data in Fig. 1. At biases $3.4\text{ V} < V_B < 5.6\text{ V}$, the zero-field capacitance is negative and with increasing bias grows in magnitude and shifts to higher frequencies. The same response occurs when the bias is fixed and magnetic field $B = 30\text{ mT}$ is applied. At $V_B > 5.6\text{ V}$, evolution of capacitance in zero field is more complicated. At $f > 100\text{ Hz}$, the capacitance continues to be negative and shifts to higher frequency with bias, whereas at $f < 10\text{ Hz}$, the capacitance reverses its sign and becomes positive. Again application of magnetic field mimics this variation: it makes the capacitance more negative at high frequencies and more positive at low frequencies.

We found that the PP model is the most natural way to explain the response of the capacitance on the magnetic field. In bipolar MEH-PPV OLEDs, a small increase in bias voltage increases the concentration of positive, n_+ , and negative, n_- , polarons. (For example, this is evident from the enhancement of electroluminescence.) Within the PP model, magnetic field has the same final effect; it decreases the rate of bimolecular recombination, allows for more carrier injection, and as a result increases n_+ and n_- . Then, the response of the system to AC electrical field (which involve several processes and can be rather complicated) simply reflects the changed carrier concentration regardless of what causes it, magnetic field, or increased bias voltage. It is interesting to notice that even though the low-frequency term C_1 is strongly affected by magnetic field, within the PP model, an elementary physical process responsible for C_1 does not need to depend on B . For example, we can assume following Bisquert *et al.*¹⁹ that C_1 is determined by the occupation of surface defects, n_S . However, n_S is in steady state equilibrium with bulk free carriers. So even though the elementary charge transfer between a surface site and a site in the bulk may not depend on B , the effect of magnetic field can occur indirectly through the magnetic field dependence of the bulk carrier concentration.

In summary, we observed magnetic-field-dependent capacitive contribution in bipolar MEH-PPV OLEDs. At low frequencies, the capacitance is divergent and sequentially changes its sign with increasing bias from positive to nega-

tive to positive again. At a certain fixed bias, the capacitance can be reversed by the magnetic field. We found the response of capacitance on the magnetic field to be consistent with the PP model of the OMAR effect.

The authors would like to thank C. Boehme, T. D. Nguyen, and Z. V. Vardeny for valuable comments and discussions. This work is supported by NSF CAREER Grant DMR 0955484, and the NSF-MRSEC program at the University of Utah, Grant No. DMR 11-21252.

- ¹J. Kalinowski, M. Cochi, D. Virgili, P. Di Marco, and V. Fattori, *Chem. Phys. Lett.* **380**, 710 (2003).
- ²O. Mermer, G. Veeraraghavan, T. L. Francis, Y. Sheng, D. T. Nguyen, M. Wohlgenannt, A. Kohler, M. K. Al-Suti, and M. S. Khan, *Phys. Rev. B* **72**, 205202 (2005).
- ³P. Desai, P. Shakaya, T. Kreouzis, and W. P. Gillin, *Phys. Rev. B* **76**, 235202 (2007).
- ⁴T. L. Francis, O. Mermer, G. Veeraraghavan, and M. Wohlgenannt, *New J. Phys.* **6**, 185 (2004).
- ⁵T. D. Nguyen, G. Hukic-Makkosian, F. Wang, L. Wojcik, X.-G. Li, E. Ehrenfreund, and Z. V. Vardeny, *Nature Mater.* **9**, 345 (2010).
- ⁶V. N. Prigodin, J. D. Bergeson, D. M. Lincoln, and A. J. Epstein, *Synth. Met.* **156**, 757 (2006).
- ⁷A. J. Schellekens, W. Wagemans, S. P. Kersten, P. A. Bobbert, and B. Koopmans, *Phys. Rev. B* **84**, 075204 (2011).
- ⁸B. Hu and Y. Wu, *Nature Mater.* **6**, 985 (2007).
- ⁹D. R. McCamey, K. J. van Schooten, W. J. Baker, S.-Y. Lee, S. Y. Paik, J. M. Lupton, and C. Boehme, *Phys. Rev. Lett.* **104**, 07601 (2010).
- ¹⁰D. R. McCamey, S.-Y. Lee, S.-Y. Paik, J. M. Lupton, and C. Boehme, *Phys. Rev. B* **82**, 125206 (2010).
- ¹¹P. Desai, P. Shakya, T. Kreouzis, W. P. Gillin, N. A. Morley, and M. R. J. Gibbs, *Phys. Rev. B* **75**, 094423 (2007).
- ¹²J. Y. Song, N. Stingelin, A. J. Drew, T. Kreouzis, and W. P. Gillin, *Phys. Rev. B* **82**, 085205 (2010).
- ¹³W. J. Baker, D. R. McCamey, K. J. van Schooten, J. M. Lupton, and C. Boehme, *Phys. Rev. B* **84**, 165205 (2011).
- ¹⁴P. A. Bobbert, T. D. Nguyen, F. W. A. van Oost, B. Koopmans, and M. Wohlgenannt, *Phys. Rev. Lett.* **99**, 216801 (2007).
- ¹⁵F. Wang, J. Rybicki, K. A. Hutchinson, and M. Wohlgenannt, *Phys. Rev. B* **83**, 241202 (2011).
- ¹⁶F. Li, L. Xin, S. Liu, and B. Hu, *Appl. Phys. Lett.* **97**, 073301 (2010).
- ¹⁷T. K. Djidjou, T. Basel, and A. Rogachev, *J. Appl. Phys.* **112**, 024511 (2012).
- ¹⁸M. Ershov, H. C. Liu, L. Li, M. Buchanan, Z. R. Wasilewski, A. K. Jonscher, *IEEE Trans. Electron Devices* **45**, 2196 (1998).
- ¹⁹J. Bisquert, G. Garcia-Belmonte, A. Pitarch, and H. J. Bolink, *Chem. Phys. Lett.* **422**, 184 (2006).
- ²⁰Y. Y. Lin, F.-M. Yang, C.-Y. Huang, W.-Y. Chou, J. Chang, and Y.-C. Lien, *Appl. Phys. Lett.* **91**, 092127 (2007).
- ²¹K. C. Kao and W. Hwang, *Electrical Transport in Solids* (Pergamon, Oxford, 1981).
- ²²M. A. Baldo and S. R. Forrest, *Phys. Rev. B* **64**, 085201 (2001).